

# Pressure Drop Characteristics of Slit-Type Heat Exchanger

**T. Ki and S. Jeong**

Cryogenic Engineering Laboratory  
Korea Advanced Institute of Science and Technology  
Korea

## ABSTRACT

A slit-type heat exchanger offers several advantages to the design of cryocoolers; it can accommodate various configurations either in a straight or tapered shape and involves no thermal contact resistance problems, which are often encountered in a mesh-type heat exchanger. The needed heat path in the radial direction of the heat exchanger of a large-scale and high-power cryocooler is especially favorable. Our focus here is on the measurement and analysis of the pressure drop characteristics of a slit-type heat exchanger. First, measurement of overall pressure drop is considered under steady-flow conditions. The analyzed parameters of the heat exchanger configuration include: 1) size of slit; 2) number of slits; and 3) angle of slit. Second, using the pressure boundary conditions obtained from the experiments, CFD (Computational Fluid Dynamics) was carried out to reproduce the experimental data. Using the CFD calculations, the entrance and exit losses of the pressure were carefully examined and identified. These results can divide the overall pressure drop into the entrance, exit, and tapered channel losses. Finally, we conclude that the pressure drop characteristics under steady flow conditions can be used for conditions of oscillating flow. The presented results should help one design an optimum regenerative cryocooler with slit-type heat exchangers.

## INTRODUCTION

A heat exchanger is one of the most important components of a cryocooler. The aftercooler and warm-end heat exchanger in a Stirling-type cryocooler should be able to dump sufficient heat and entropy to the outside for the cryocooler to reach a desirable low temperature. A cold-end heat exchanger needs to be carefully designed for satisfying the required performance and temperature stability between the gas and the heat exchanger at the cryogenic temperature. It is important to know the flow and the heat transfer characteristics of the heat exchangers for optimal design of cryocoolers.

A slit-type heat exchanger has several advantages.<sup>1-5</sup> If a slit-type heat exchanger is employed as a straight or tapered shape, cryocoolers having different flow cross-sections around the aftercooler, cold-end, and warm-end heat exchanger can have smooth flow transitions. The slit-type heat exchanger also has no thermal contact resistance problems that are often encountered with a mesh-type construction, and the appropriate heat path in the radial direction in a large scale and high-power PTR is especially favorable. Although the optimal design of a pulse tube refrigerator with slit-type heat exchangers necessitates knowledge of their flow and heat transfer characteristics,

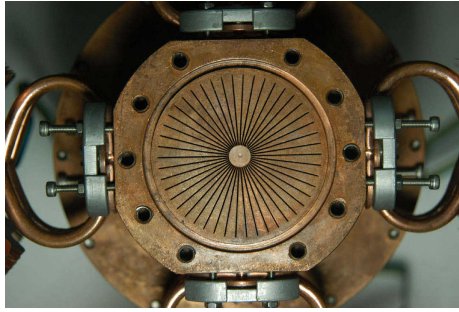


**Figure 1.** Slit-type heat exchanger.

there is little research that has been conducted for such a purpose. Only a parallel rectangular channel approximation has been used to characterize a slit-type heat exchanger in a design process. The characteristics of slit-type heat exchangers are quite different from those of parallel rectangular channels in that a slit-type heat exchanger has both radially dispersed and axially tapered channel effects. Especially in the region around the entrance, tapered channel, and exit, the characteristics of pressure drop must be significantly different from that of a parallel rectangular channel.

In this paper, pressure drop characteristics of slit-type heat exchanger are investigated through flow measurements and CFD analysis. For various configurations of slit-type heat exchangers, each pressure drop has been measured under steady flow conditions. Measurements in both the positive and negative flow directions have been conducted in consideration of the conditions of oscillating flow. The measured pressure drop has been decoupled by entrance, tapered channel, and exit loss using CFD. Finally, we show that the pressure drop characteristics of steady flow can be used for oscillating flow by considering the acoustic impedance of slit-type heat exchangers.

## PRESSURE DROP COMPONENTS

A typical installation of a heat exchanger involves flow contraction and expansion at the core entrance and exit. This frontal flow area change complicates the characteristics of flow-stream pressure drop. Since cryocooler designers are usually interested in the overall pressure drop of the heat exchanger, rather than the specific local core friction pressure drop, it is useful and informative to understand how the overall pressure drop is distributed along the heat exchanger assembly. In the case of a regenerative cryocooler design where the system pressure is oscillating, the entrance and exit effects are important in the whole design process. The amplitude of the entrance and exit losses cannot be ignored in comparison with the core loss of the heat exchanger, and also asymmetric characteristics of the entrance and exit effects can generate DC flow in a pulse tube cryocooler. It is, therefore, necessary to examine the overall pressure drop and identify each pressure drop component for optimal design of cryocoolers.

For steady flow, a typical pressure drop curve of a heat exchanger with rectangular channels is depicted in Fig. 2. It is separated by the entrance, channel, and exit parts.<sup>6</sup> If the heat exchanger has a symmetric configuration at the entrance and exit regions, the pressure drop characteristic is the same regardless of the flow direction. However, a slit-type heat exchanger has usually an asymmetric configuration because the tapered channel height changes along the channel length to accommodate different flow cross-sections in adjacent components of a cryocooler.<sup>7,8</sup> For complete understanding of pressure loss under oscillating flow conditions, the pressure drop in both flow directions should be known and decoupled in the entrance, exit, and tapered channel regions as shown in Fig. 3.

The overall pressure drop of slit-type heat exchangers having different number, angle, and size of the slit have been measured under steady flow conditions in both flow directions. By using the pressure drop measurements as the boundary conditions, CFD analysis has also performed. The CFD analysis enables one to decouple the entrance, tapered channel, and exit losses, respectively.

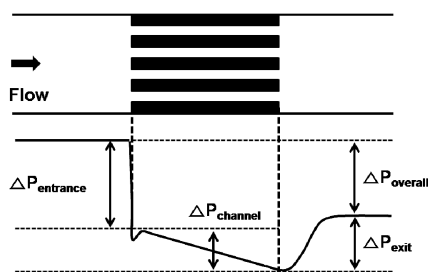


**Figure 2.** Pressure drop components in a heat exchanger channel.

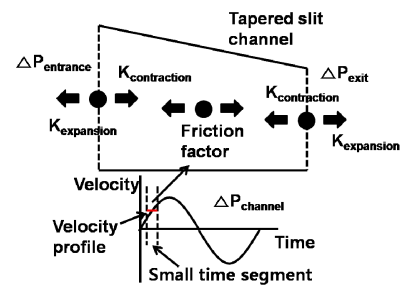


**Figure 3.** Schematic of pressure drop components in the oscillating condition.

The analysis helps one understand the flow characteristic around the heat exchanger in both flow directions. The obtained entrance and exit losses under steady flow conditions are applied to oscillating pressure and flow conditions after the pressure drop of the tapered channel is checked with respect to the phase change that is generated by the compliance effect.

**EXPERIMENTAL SETUP AND SLIT-TYPE HEAT EXCHANGERS**

The experimental apparatus used in this research is shown schematically in Fig. 4. Static pressure sensors (Honeywell®) and differential pressure sensors (Validyne® DP15) are used for measuring the overall pressure drop between the slit-type heat exchangers. Two static pressure sensors are for measuring entry static pressure according to the flow direction. The overall pressure drop is measured by an outer differential pressure sensor and this result is used for the pressure boundary conditions of the CFD simulation. The overall pressure drop measured by the inner differential pressure sensor is used for confirming the CFD simulation results. We have employed a liquid nitrogen tank and its evaporator to supply the desired mass flow rate in the range of 10 g/s, and we continuously maintain the charge pressure using a regulator. The mass flow rate is measured and controlled by a Coriolis mass flow meter (MaxFlo®) and a needle valve (Swagelok®). Temperature as well as pressure are monitored during an experiment in order to calculate nitrogen gas density. Measured data are saved by a Data Acquisition System (DAS) for archival purposes.

Six slit-type heat exchangers with different configurations as shown in Fig. 5 and tabulated in Table 1 were used in the experiments. These are all copper blocks with tapered slit channels, and each has a diameter change from the entrance to the exit region to match standardized tube diameter sizes (2.25 inch, 1.25 inch, 1 inch and 0.5 inch) used for typical linear-compressor cylinder, regenerator, and pulse tube construction. After making a small hole in the copper block center using a super drill, the tapered slits in the heat exchanger are fabricated by Electrical Discharge Machining (EDM). The small center hole is later blocked by a machined brass bar.

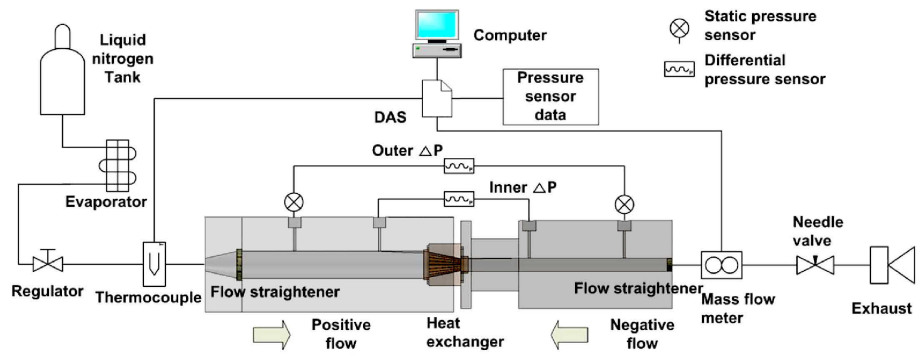


**Figure 4.** Experimental apparatus for steady flow measurements.

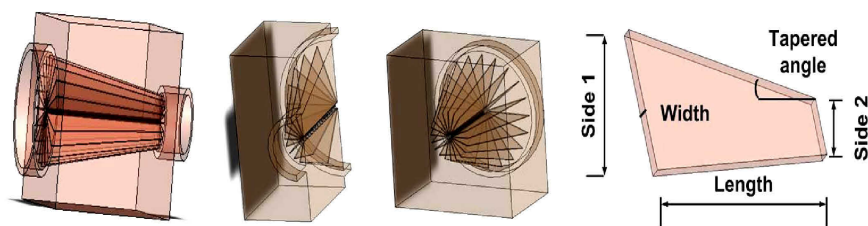


Figure 5. Configurations of slit-type heat exchangers.

Table 1. Specification of slit-type heat exchangers

Heat exchanger	Inlet height (mm)	Outlet height (mm)	Width (mm)	Slit number	Length (mm)	Tapered angle (Degree)
1	25.9	13.6	0.33	18	112	6.3
2	23.9	11	0.46	46	50	14.5
3	26	10.5	0.38	20	112	7.9
4	14.1	4.4	0.38	20	25	21.3
5	11	4.7	0.35	20	30	11.9
6	10.5	10.5	0.37	20	40	0

CFD

The CFD simulation program, Fluent®, was used to separate the effects attributable to the individual pressure drop components in the tapered slit-type heat exchangers. Symmetry was used to allow each slit-type heat exchanger to be modeled for computation purposes by a single slit as shown in Fig. 6. All grids were carefully created and tested with Gambit in three dimensions to insure the generation of high quality grids in slits having a very large aspect ratio. All computational models used a pressure-based numerical solver for the steady state condition and employed a second order upwind method control scheme with a SIMPLE pressure-velocity coupling. As a result of the high Reynolds number observed in the tapered slit channel and in the extended inlet and outlet regions, a realizable  $k-\varepsilon$  turbulence model was applied. In all cases, inlet and outlet pressure boundary conditions measured from the experiments were used, and pressure gradients were calculated in the tapered slit-type heat exchangers. From the calculated results, each pressure drop component was separated and characterized by its friction factor, entrance, and exit loss coefficients as follows.<sup>6</sup>

$$\begin{aligned}\Delta P_{contraction} &= \frac{G^2}{2\rho}(1-\sigma^2 + K_c) \\ \Delta P_{expansion} &= \frac{G^2}{2\rho}(1-\sigma^2 - K_e) \\ \Delta P_{channel} &= \frac{G^2}{2\rho} \frac{4L}{D_h} f\end{aligned}\tag{1}$$

- where,
- $D_h$  is the hydraulic diameter
  - $f$  is the friction factor
  - $G$  is the mass velocity
  - $L$  is the channel length
  - $K_c$  is the contraction loss coefficient
  - $K_e$  is the expansion loss coefficient
  - $\sigma$  is the ratio of free flow area

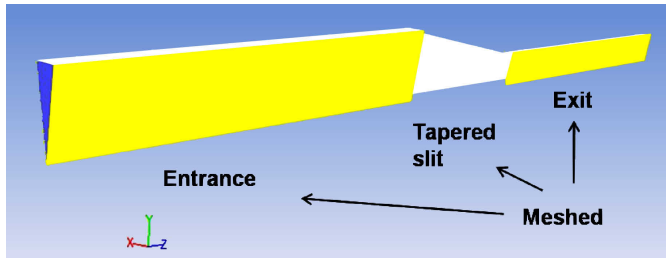


Figure 6. Configuration and mesh in the tapered slit channel.

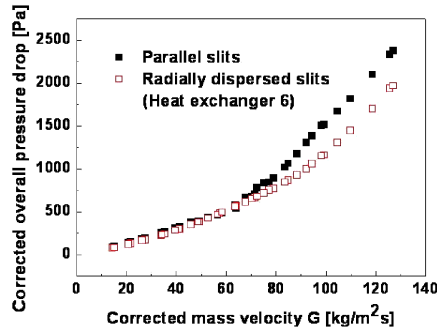


Figure 7. Difference of corrected overall pressure drop between parallel and radially dispersed slit channels with the ratio of free flow area (0.15) and same slit configuration

## EXPERIMENTAL AND CFD RESULTS

Experiments were conducted with parametric charge pressures of 10, 7 and 5 bars. To normalize the experiment temperature and charge pressure conditions, we corrected all the measurement results for the density and dynamic viscosity at standard conditions (10 bar, 15°C).<sup>9</sup>

Fig. 7 clearly shows that there is a difference of the corrected overall pressure drop between the radially dispersed (heat exchanger 6) and the usual parallel rectangular channels. In parallel rectangular channels, each pressure drop of entrance, exit, and channels is obtained from the data of Shah and Bhatti (1987).<sup>9</sup> The two heat exchangers have the same width, height, length, and number of channels, but the direction of the slits is different. This can induce different characteristics of entrance and exit losses. Fig. 7 shows this effect, and we realize that the radially dispersed slits have less entrance and exit losses, especially at high mass velocity. Therefore, it is concluded that the previous general correlation of parallel channels cannot be used for the radially dispersed channels. We need further investigation on the pressure drop for the radially dispersed slit channels.

Fig. 8 shows the corrected overall pressure drop of tapered slit-type heat exchangers 1-5. From these results, we find a substantial dependency of pressure drop on the flow direction. Especially, the tapered slit-type heat exchangers with short length (heat exchanger 4 and 5) display a large pressure difference between positive and negative flows. This means that the entrance, the exit, and the tapered angle effects that generate asymmetric characteristics are dominant in these cases. The difference, therefore, has to be carefully considered for design of tapered slit-type heat exchangers having a relatively short length (especially, the cold-end heat exchanger) because the combined and accumulated asymmetric effect may generate a secondary flow loss in cryocoolers.

For ease of understanding the overall characteristics of the tapered slit-type heat exchanger, overall friction factors are shown in Fig. 9. The overall friction factors contain all pressure drop components including entrance and exit losses because these effects cannot be easily decoupled. The Reynolds number ( $Re$ ) in Fig. 9 is based on the short slit side. From these results, we can easily confirm that the higher friction factors lead to large differences between positive and negative flow.

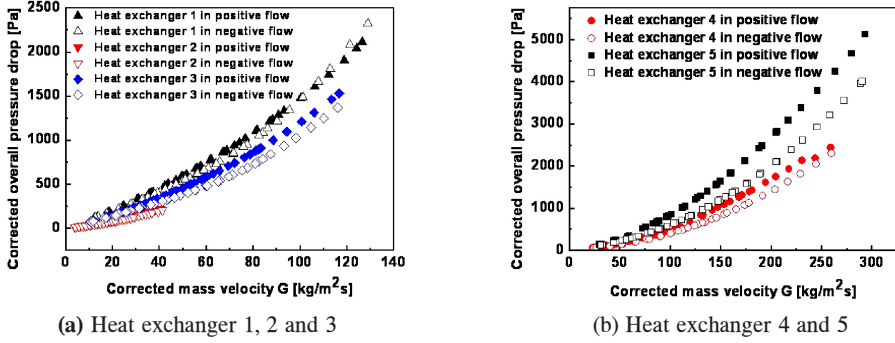


Figure 8. Corrected overall pressure drop in tapered slit-type heat exchangers

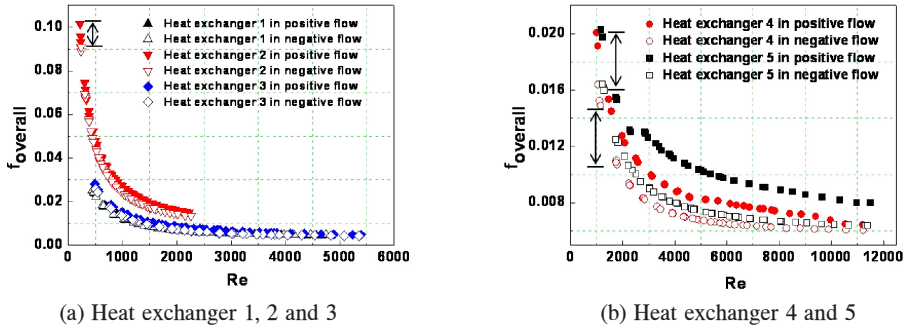


Figure 9. Overall friction factors in tapered slit-type heat exchangers.

This means that high friction factor or low Reynolds number conditions can induce larger asymmetric characteristics of pressure drop. Since the experimental cases have different overall friction factor curves, nondimensional parameters are used for generalizing the overall friction factor.

The taper angle ( $\theta$ ) and the ratio of the free flow area to the frontal and back area ( $\sigma_{inlet}$ ,  $\sigma_{outlet}$ ), which embody the width, height, and number of slits in the heat exchanger, are considered in the definition of the overall friction factor as follows:

Positive flow

$$f_{overall} = 17.8(\text{Re} - 32.4)^{-0.73} (3.3 + \theta)^{-0.108} \sigma_{inlet}^{0.59} \sigma_{outlet}^{0.12} \quad \text{Re} < 4000$$

$$f_{overall} = 1.3(\text{Re} - 1)^{-0.3} (1 + \theta)^{-0.102} \sigma_{inlet}^{1.04} \sigma_{outlet}^{0.003} \quad \text{Re} \geq 4000$$

Negative flow

$$f_{overall} = 40.42(\text{Re} - 44.15)^{-0.8} (14.6 + \theta)^{-0.19} \sigma_{inlet}^{0.79} \sigma_{outlet}^{-0.093} \quad \text{Re} < 4000$$

$$f_{overall} = 0.284(\text{Re} - 1)^{-0.23} (4.9 + \theta)^{-0.11} \sigma_{inlet}^{0.55} \sigma_{outlet}^{0.23} \quad \text{Re} \geq 4000$$

(2)

Fig. 10 shows the accuracy of the correlated overall friction factors. In this generalized overall friction factor, the positive and the negative flow correlations have maximum errors of 8% and 15%, respectively.

Realizing the difficulty of applying the overall friction factor for diverse slit-type heat exchangers, we tried to decouple the genuine effect of pressure drop due to the tapered slit from the entrance and exit losses. Fig. 11 and Fig. 12 show the CFD results for heat exchanger 4 for positive flow conditions. The individual entrance and exit loss trends are similar to those for the parallel

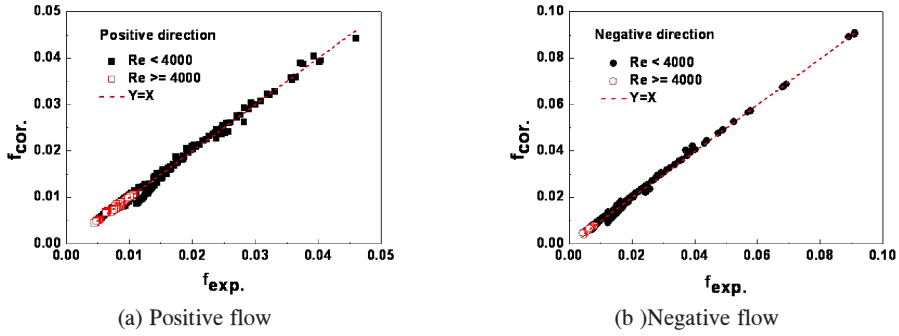


Figure 10. Accuracy of correlated overall friction factors.

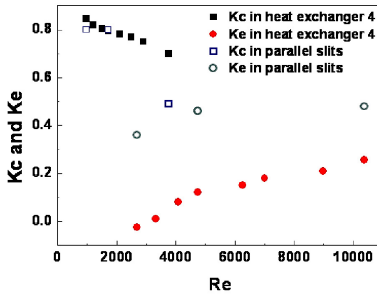


Figure 11. Divided entrance and exit losses.

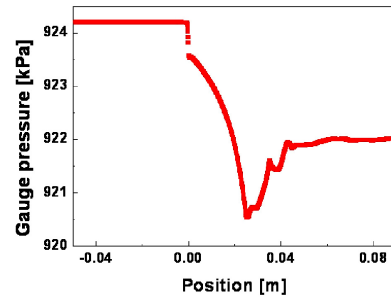


Figure 12. Pressure drop curve from CFD.

rectangular slits, but the amplitudes of the entrance and exit losses are different. Especially, the exit losses always have a small amplitude, and the entrance losses have a large amplitude for increasing Reynolds numbers. This means that the effect due to the tapered angle and the radially dispersed slits is important. Since the tapered slit channels with large aspect ratios require a very large grid number for CFD, the CFD simulation with the turbulent model consumes a huge amount of time for obtaining accurate results. The CFD simulation could not be completed for all heat exchanger cases; a more efficient method is necessary.

## APPLICATION FOR OSCILLATING FLOW CONDITIONS

It may be questioned if the steady-flow correlation obtained in the previous section is useful for the oscillating flow conditions in a cryocooler design. This section specifically considers the efficacy of the steady pressure drop correlation of the slit-type heat exchanger in the view of an acoustic impedance model. An acoustic impedance model for oscillating gas flow in rectangular channels is commonly used for the design and analysis of harmonic systems. Generally, the acoustic impedance of a slit is the ratio of complex amplitudes of pressure drop to volumetric flow rate and can be expressed with resistive and reactive parts.

$$Z = \frac{\Delta P}{U} = r + xj \quad (3)$$

The acoustic impedance can be further notated by electrical elements as follows:

$$Z = R + j(\omega L - 1/\omega C) \quad (4)$$

where  $R$ ,  $L$ , and  $C$  are the acoustic resistance, inertance, and compliance of the equivalent hydraulic system. According to previous research, these impedances are analyzed as follows, and in the case of a rectangular channel the impedance becomes<sup>10</sup>



$$Z = \frac{-(i\omega\rho/ad)(1-i)Y}{\tan\{(1-i)Y\} - (1-i)Y} = (b\omega\rho/ad) \times r(f(Y)) + i(b\omega\rho/ad) \times x(f(Y)) \quad (5)$$

$$f(Y) = [-(1-i)Y] / [\tan\{(1-i)Y\} - (1-i)Y]$$

where,

- $a$  is the long dimension of the channel cross section
- $d$  is the narrow dimension of rectangular channel cross section
- $L$  is the geometric rectangular channel length
- $Y$  is  $\pi$  times the ratio of  $d$  to the viscous wavelength
- $\rho$  is density of the gas
- $\omega$  is radian frequency

In small rectangular channels where the high-aspect ratio approximation is applicable, the impedance can be written as follows<sup>11</sup>

$$Z = \frac{-\mu L \pi^2}{32b^4} \left[ \sum_{n=0}^{\infty} \frac{1}{(2n+1)^2 q_n^2} \left( \alpha - \frac{\tanh(q_n \alpha)}{q_n} \right) \right]^{-1} = r + i\omega x \quad (6)$$

$$q_n = \sqrt{i\eta^2 + \frac{(2n+1)^2}{4} \pi^2}$$

where,

- $b$  is the channel half-height
- $\alpha$  is the channel aspect ratio
- $\eta$  is the nondimensional frequency parameter
- $\mu$  is the dynamic viscosity

The impedance of slit channels with a small void volume does not have a significant compliance effect because the gas moves almost simultaneously at the inlet and exit. Therefore, the change in pressure phase angle across a slit-type heat exchanger is not significant, as illustrated in Fig. 13. Only the resistance part is meaningful in the pressure drop characteristic, even for most oscillating flow conditions in regenerative cryocoolers. As shown in Fig. 3, a tapered channel can be divided into three parts: entrance, exit, and channel regions. If the overall pressure losses obtained from the steady flow condition can be generalized according to flow, the pressure drop of the tapered slit-type heat exchanger can be derived for oscillating flow conditions, regardless of the gas stroke. First, each time-averaged pressure drop generated from the entrance and the exit regions over a cycle is obtained from Eq. (7).<sup>7</sup>

$$\Delta P = \frac{\rho u_{max}^2}{8} (K_{contraction} - K_{expansion} - 2) \quad (7)$$

Second, at each small incremental time segment of the cycle, the velocity profile of particle segments in the tapered channel region can be considered to be constant. If we know the friction factor, which is obtained from the steady flow condition at this temporal velocity or Reynolds number, the pressure loss in the tapered channel can be calculated during this time segment. Therefore, the total pressure drop of the gas during a total stroke can be obtained by combining the channel loss integrated over the cycle with losses for the entrance and exit regions.

## SUMMARY

The pressure drop characteristics of a slit-type heat exchanger with radially dispersed and tapered slits have been studied for both steady and oscillating flow conditions. First, for steady flow conditions, the overall pressure drop of six tapered slit-type heat exchangers with different slit configurations was measured for both flow directions, and the overall friction factors were obtained. From these results, asymmetric pressure drop characteristics and different overall friction factors were derived for each configuration of the slits and flow direction. The generalized new overall friction factor is presented with maximum errors of 8 % and 15 % according to the flow



direction. Second, CFD simulation, which allowed dividing the overall pressure drop into entrance, exit, and channel losses, was conducted to obtain a more accurate correlation. Finally, the acoustic impedance method was appealed to to confirm the applicability of using the steady-flow experimental data for the oscillating-flow conditions that commonly occur in regenerative cryocoolers. The pressure drop characteristics of the slit-type heat exchanger investigated in this paper should be useful for the optimum design of large-capacity pulse tube refrigerators.

## ACKNOWLEDGMENT

This work was supported by the Korea Science and Engineering Foundation (KOSEF) grant funded by the Korea government (MOST) (No. R0A-2007-000-20062-0).

## REFERENCES

1. Ki, T. and Jeong, S., "Optimal Design of Pulse Tube Refrigerator with Slit-type Heat Exchangers," *Proc. of the 23th Space Cryogenics Workshop*, Cryogenic Society of America, 2009, pp. 231-241.
2. Ki, T. and Jeong, S., "Stirling-type pulse tube refrigerator with slit-type heat exchangers for HTS superconducting motor," To be presented at the Asian Conference on Applied Superconductivity and Cryogenics 2009, Matsue, 2009.
3. Ercolani, E., Poncet, J. M., Charles, I., Duband, L., Tanchon, J., Trollier, T., Ravex, A., "Design and prototyping of a large capacity high frequency pulse tube," *Cryogenics*, Vol. 48, No. 9-10 (2008), pp. 439-447.
4. Su, W., Ju, Y. L., Chen, M., "Development of miniature coaxial pulse tube cryocooler with novel integral cold finger," *Proceedings of ICEC 22* (2008), pp. 549-554.
5. Mohanta, L. and Atrey, M. D., "Experimental investigation of single-stage in-line Stirling-type pulse tube refrigerator," *Cryocoolers 15*, ICC Press, Colorado (2009), pp. 185-189.
6. Kays, W. M. and London, A. L., *Compact heat exchangers*, McGraw-Hill, New York (1984).
7. Smith, B. L. and Swift, G. W., "Power dissipation and time-averaged pressure in oscillating flow through a sudden area change," *J. Acoust. Soc. Am.*, Vol. 113, No. 5 (2003), pp. 2455-2463.
8. Petculescu, A. and Wilen, B. L., "Oscillatory flow in jet pumps: nonlinear effects and minor losses," *J. Acoust. Soc. Am.*, Vol. 113, No. 3 (2003), pp. 1282-1292.
9. Shah, R. K. and Sekulic, D. P., *Fundamentals of heat exchanger design*, Wiley, New Jersey (2003).
10. Thurston, G. B. and Wood, J. K., "Acoustic impedance of rectangular tubes," *J. Acoust. Soc. Am.*, vol. 25, No. 5 (1953), pp. 858-860.
11. Christopher, J. M. and Fred, K. F., "The correct treatment of harmonic pressure-flow behavior in microchannels," *Proceedings of the ASME IMECE*, vol. MEMS-2, Orlando (2000), pp. 473-479.

